

AN ABSTRACT OF THE THESIS OF

Frank Tefft Churchill for the M. S. in E. E.
(Name) (Degree) (Major)

Date thesis is presented August 14, 1964

Title AN ELECTROLYTIC TANK ANALOG FOR
MYOELECTRIC SURFACE POTENTIALS

Abstract approved 
(Major professor)

It was observed that certain myoelectric surface potentials are of a pulse nature. The pulses have nearly the same exact waveshape, but are asynchronously repetitive.

Physiological evidence indicated that myoelectric pulses are concurrent with the activity of a small unit of organized muscle fibres (motor unit). The electrical activity of the motor unit was the basis for the design of a simple electrolytic tank electrode system.

A set of myoelectric surface potential waveforms derived from multiple-point observations were used to establish geometrical relationships which were incorporated in the electrolytic tank analog. The electrolytic tank analog was then able to produce waveforms whose general characteristics corresponded quite well to the given set of myoelectric waveforms.

AN ELECTROLYTIC TANK ANALOG FOR
MYOELECTRIC SURFACE POTENTIALS

by

FRANK TEFFT CHURCHILL

A THESIS

submitted to

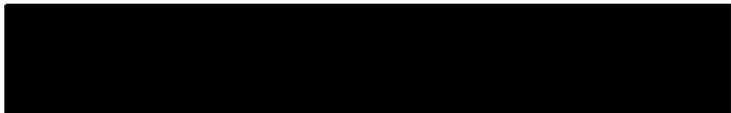
OREGON STATE UNIVERSITY

in partial fulfillment of
the requirements for the
degree of

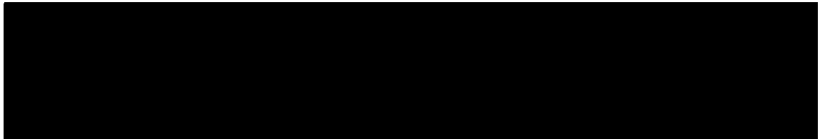
MASTER OF SCIENCE


August 1964

APPROVED:


Associate Professor of Electrical Engineering

In Charge of Major


Head of Department of Electrical Engineering


Dean of Graduate School

Date thesis is presented August 14, 1964

Typed by Norma Hansen

ACKNOWLEDGEMENT

The Author is indebted to:

R. R. Michael for his help and guidance,
J. M. Comstock and J. Blank for their criticisms,
and his wife, Jean, for her help and understanding.

The experimental portions of this work were made possible by financial support of the Engineering Experiment Station and the Graduate Research Council, both of Oregon State University, and by a generous contribution of equipment from the Tektronix Foundation, Beaverton, Oregon.

TABLE OF CONTENTS

	Page
INTRODUCTION	1
PRELIMINARY STUDIES	2
Myoelectric Surface Potentials	2
Muscle Fibres	11
Motor Units	13
Hypothesis	14
EXPERIMENTAL STUDIES	15
Analog Characteristics	15
Electrolytic Tank Fabrication	21
Myoelectric Data Acquisition	24
Motor Point Location	31
Procedure	36
Results	36
CONCLUSION	40
BIBLIOGRAPHY	43

LIST OF FIGURES

	Page
1. Random Myoelectric Waveforms	3
2. Myoelectric Pulse Waveforms	4
3. Biphasic and Monophasic Pulse Waveforms	6
4. Electrode Placement for Monopolar and Differential Recording	7
5. Repetitive Single Point Myoelectric Waveforms	9
6. Repetitive Multiple-Point Myoelectric Waveforms	10
7. Representative Section of a Muscle Fibre . .	12
8. Membrane Potential Difference	12
9. Geometry for the Mathematical Analog	16
10. Typical Waveform Generated by the Mathematical Analog	19
11. Signal Flow Diagram for AC Carrier System. .	23
12. Typical Electrolytic Tank Waveform	25
13. Differential Electrode Array	26
14. Monopolar Electrode Array	27
15. Superimposed Tracings of Myoelectric Waveforms	29
16. Tracing of Averaged Differential Myoelectric Waveforms	30
17. Tracing of Averaged Monopolar Myo- electric Waveforms	32

LIST OF FIGURES (Continued)

	Page
18. Superimposed Tracings of Differential Myoelectric Waveforms (Subject No. 2) . . .	34
19. Superimposed Tracing of Monopolar Myoelectric Waveforms (Subject No. 2) . . .	35
20. Comparison of Differential Myoelectric and Analog Waveforms	37
21. Comparison of Distal Monopolar Myo- electric and Analog Waveforms	38
22. Comparison of Proximal Monopolar Myo- electric and Analog Waveforms	39

AN ELECTROLYTIC TANK ANALOG FOR MYOELECTRIC SURFACE POTENTIALS

INTRODUCTION

Recently, interest has been expressed regarding the application of myoelectric phenomena to machine control (12, 16, 20). A basic requirement for such control is a suitable language (code) that will allow reliable communication between man and machine (15). Implicit in the generation of such a code is knowledge of the fundamental processes involved. The exploitation of myoelectric surface potentials requires definition of the relationship between myoelectric surface potentials and their generating mechanisms.

One approach for defining the relationship between two sets of phenomena involves the construction of an analog. A suitable analog for relating myoelectric phenomena to their generating mechanisms would be an electrolytic tank analog. Consequently, the objective of this work is to construct an electrolytic tank analog on the basis of concepts derived from observations and to evaluate it with respect to the correlations between myoelectric phenomena and their generating mechanisms.

Precise correlations will not be required for achievement of the objectives. An electrolytic analog should be capable of generating characteristic signals consistent with those observed. The resulting information should contribute to the development of a myoelectric language.

PRELIMINARY STUDIES

Myoelectric Surface Potentials

Myoelectric surface potentials are electric potentials occurring on the surface of the skin which are generally thought to coincide with the excitation of muscle fibres (7). The amplitudes of these signals are quite small (10-1000 μ v), and their frequency spectrum ranges from 20 to 8000 cps (18, p. 46). Instrumentation of myoelectric surface potentials is difficult and numerous investigators have examined this problem of electrodiagnostic procedure (6, 8, 17).

Typical myoelectric waveforms are displayed in Figures 1 and 2. Comparison of these two electromyograms reveals two waveforms with different properties. The waveform in Figure 1 seems to be random in both amplitude and time, whereas the waveform in Figure 2 consists of similar

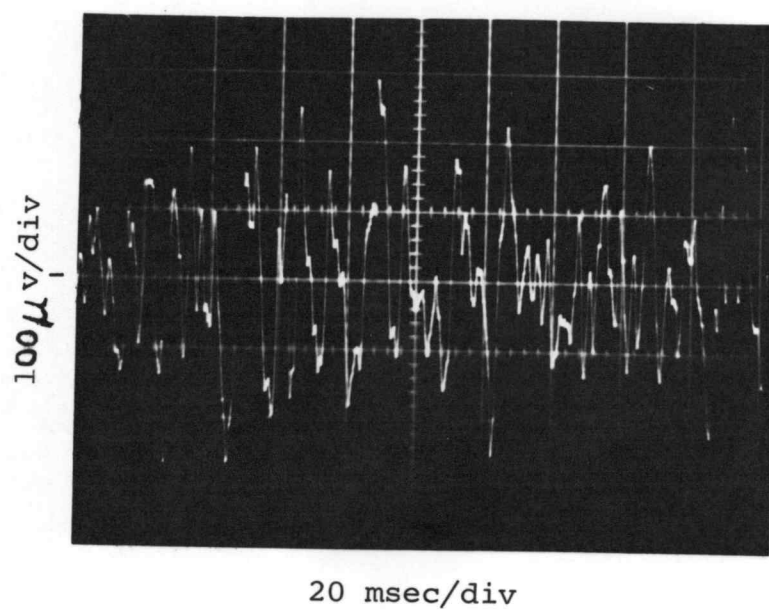


FIGURE 1

Random Myoelectric Waveforms

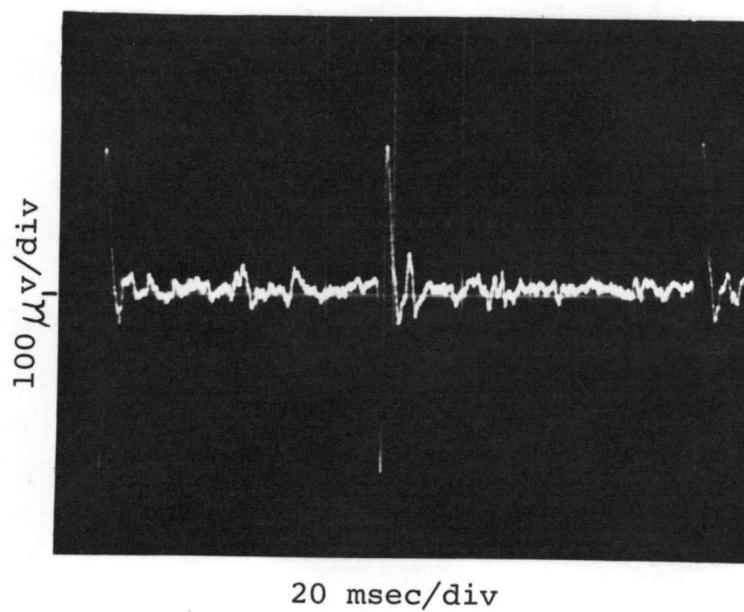


FIGURE 2

Myoelectric Pulse Waveforms

pulses in an asynchronously repetitive sequence. Clearly, analysis of the type of signals represented by Figure 2 should be more straightforward than analysis of those signals represented by Figure 1.

The pulse waveform is dependent upon, among other factors, the position of the sampling electrodes and upon the recording technique used (9). The top and middle traces in the photograph of Figure 3 contain biphasic pulses; whereas, the bottom trace contains monophasic pulses. Biphasic and monophasic pulses are characteristic of differential and monopolar recordings respectively.

The distinction between monopolar and differential recording is illustrated in Figure 4. Monopolar recording is implemented by placing two electrodes on the surface; one (the active electrode) is placed directly over the active myoelectric area (point A), and one (the indifferent electrode) is placed remote from the active area (point B). The potential of point B is assumed to remain constant (equal to the potential of all points in the absence of myoelectric activity). Consequently, the potential difference between points A and B is the dynamic potential at point A with reference to the rest potential

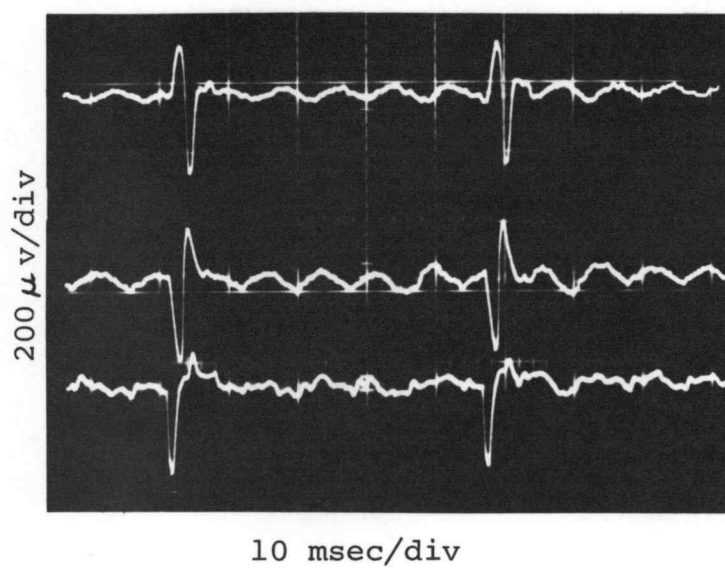


FIGURE 3

Biphasic and Monophasic
Pulse Waveforms

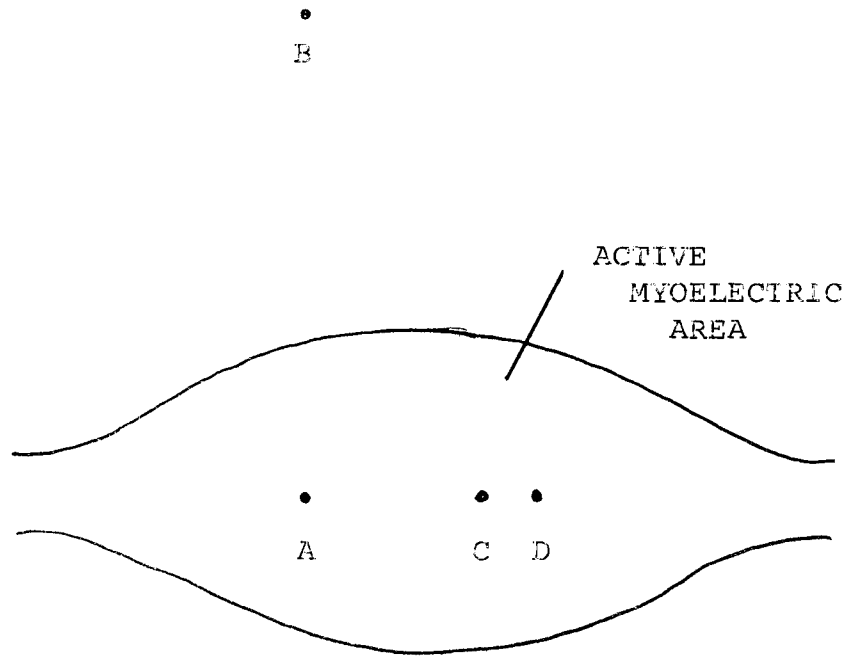


FIGURE 4

Electrode Placement for
Monopolar and Differential Recording

of the flesh. Differential recording differs from monopolar recording in that the two electrodes are placed closely together over the active area (points C and D). The resultant potential difference is the average directional derivative of the potentials of points in between the two electrodes.

Although pulse waveshape varies when sampled at different points and is a function of the recording method used, there is a striking similarity among pulses observed at a single point with a given recording method. This similarity is demonstrated in the photograph of Figure 5, which was obtained by holding the camera shutter open for multiple exposure while the oscilloscope was being triggered at some level on the leading edges of the pulse waveforms. Clearly, the waveforms thus observed are nearly identical, though the portion of the waveforms preceding the trigger point cannot be viewed with this method.

Figure 6 displays four signals that were sampled simultaneously at four different differential pairs of points. These signals have generally the same characteristic waveshape, and a time shift is evident among the

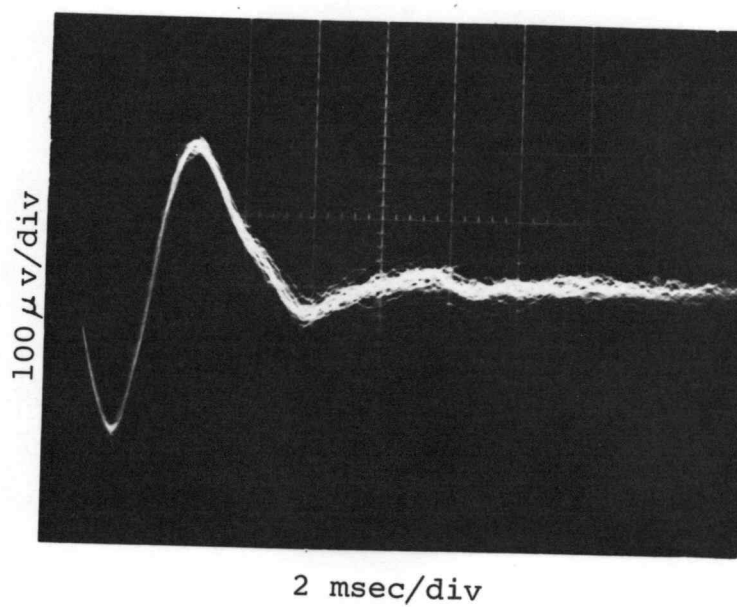


FIGURE 5

Repetitive Single Point
Myoelectric Waveforms

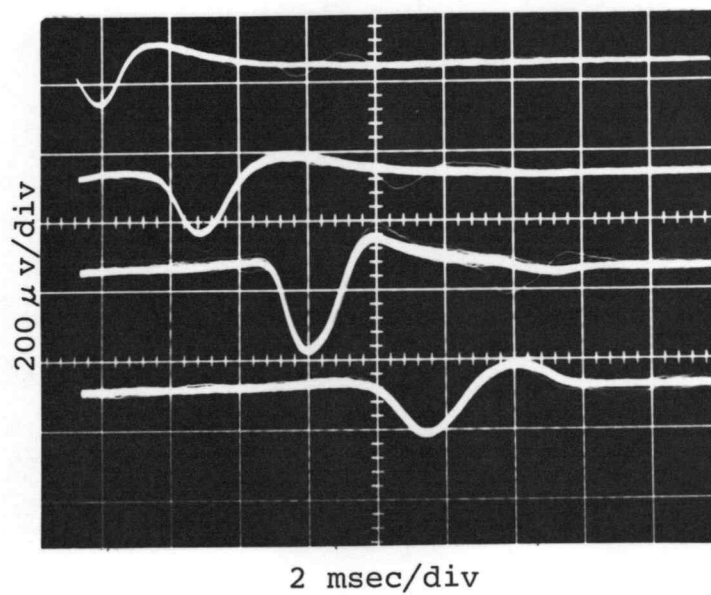


FIGURE 6

Repetitive Multiple-Point
Myoelectric Waveforms

pulse waveforms sampled at different points. Inasmuch as the same photographic technique was used as in Figure 5, the time shift is clearly a consistent property of the myoelectric signals sampled at different points.

Such similarity of waveform and consistent time shift would lead one to expect a myoelectric generating mechanism to function in a coherent manner.

Muscle Fibres

The fundamental unit of human skeletal muscle structure is the muscle fibre (cell). A muscle fibre is generally continuous for the length of the anatomical muscle (up to 30 cm), and will have a diameter of 10-100 μ (14; 22, p. 26). Normally, each fibre is innervated near the center of its length by a branch of a motor neuron (5).

Innervation involves the electrochemical response of a muscle fibre to stimulation by a motor neuron branch (1, 19). A diagram of this response is given in Figure 7. When the fibre is at rest, there exists a potential difference of about 70 mv across the cell membrane due to the ionic permeability of the cell membrane. Excitation of the motor neuron branch results in an electrochemical

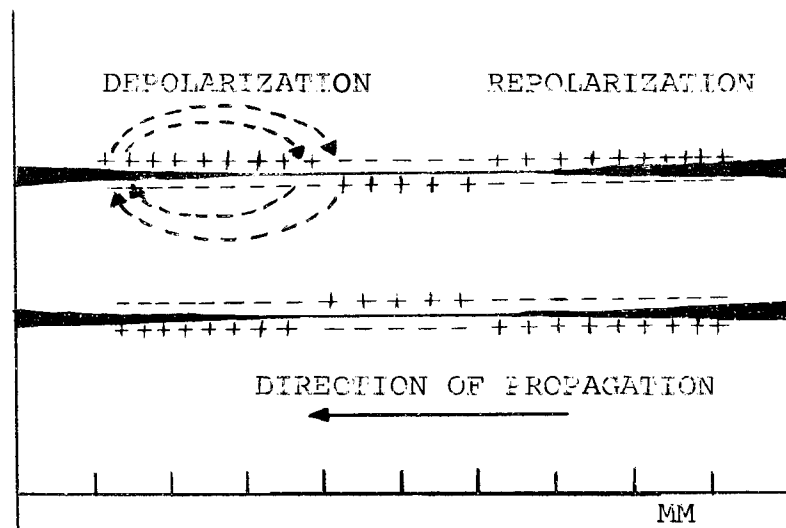


FIGURE 7

Representative Section of a Muscle Fibre

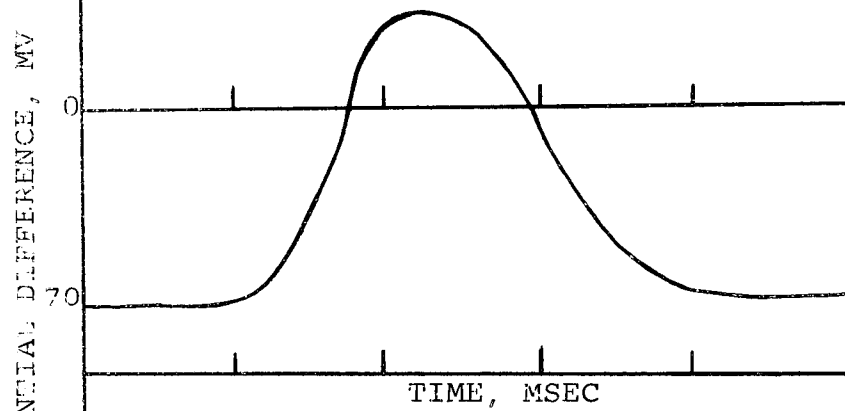


FIGURE 8

Membrane Potential Difference

process at the motor end plate which in turn initiates a discharge of the potential difference at that point. The resultant ionic flow induces breakdown in adjacent areas of the membrane, initiating the propagation of depolarization wavefronts toward both ends of the fibre. Subsequent to the depolarization of a point on the membrane, a repolarization occurs, restoring it to the initial rest potential difference. Consequently, repolarization wavefronts follow those of depolarization, resulting in the propagation of ionic current sources (charge disturbances) from the initial excitation point to the ends of the fibre. Figure 8 depicts the potential difference at a point on the membrane as a function of time during the depolarization and repolarization processes (7).

Motor Units

The anatomical entity, consisting of a motor neuron axon and all its branches and all muscle fibres innervated by the branches, is termed a motor unit (7). The muscle fibres of a motor unit are interleaved with fibres of other motor units; consequently, the effective diameter of the motor unit may be as large as 11 mm (3, p. 14).

The fibres of a motor unit are more or less mutually parallel; however, the motor end plates do not necessarily lie in a given cross-sectional plane (5). Assuming

- (1) The motor end plates all lie within a narrow cylindrical section;
- (2) All fibres are excited simultaneously;
- (3) The propagation velocities of charge disturbances in different fibres are the same;

then the myoelectric signals associated with a motor unit will differ only in amplitude from the signals produced by a single fibre. In other words, the motor unit will operate in the traveling charge disturbance mode of a muscle fibre. These approximations may be invalid for certain classes of muscles (5). However, realistic implementation of an elementary analog requires the use of these approximations.

Hypothesis

The hypothesis was that the time and waveshape characteristics of myoelectric signals could be represented by a suitable analog containing some model of the traveling charge concept.

EXPERIMENTAL STUDIES

Analog Characteristics

Consideration of the hypothesis and preliminary studies suggested two analogs: (1) a mathematical potential field analog, and (2) an electrolytic tank analog. The two analogs were developed in that order.

The geometrical relationships necessary for mathematical analysis are displayed in Figure 9. Several basic assumptions are made:

- (1) The motor unit operates in a moving charge disturbance mode which can be represented by a line current source with moving point current sources superimposed on the line source;
- (2) The volume conductor is isotropic;
- (3) Only the conduction field contributes to the potential phenomena;
- (4) The boundary representing the surface is an insulating plane whose elements are parallel to the line source.

The line source is placed on the x axis with the coordinate origin, which serves as the starting point for the two

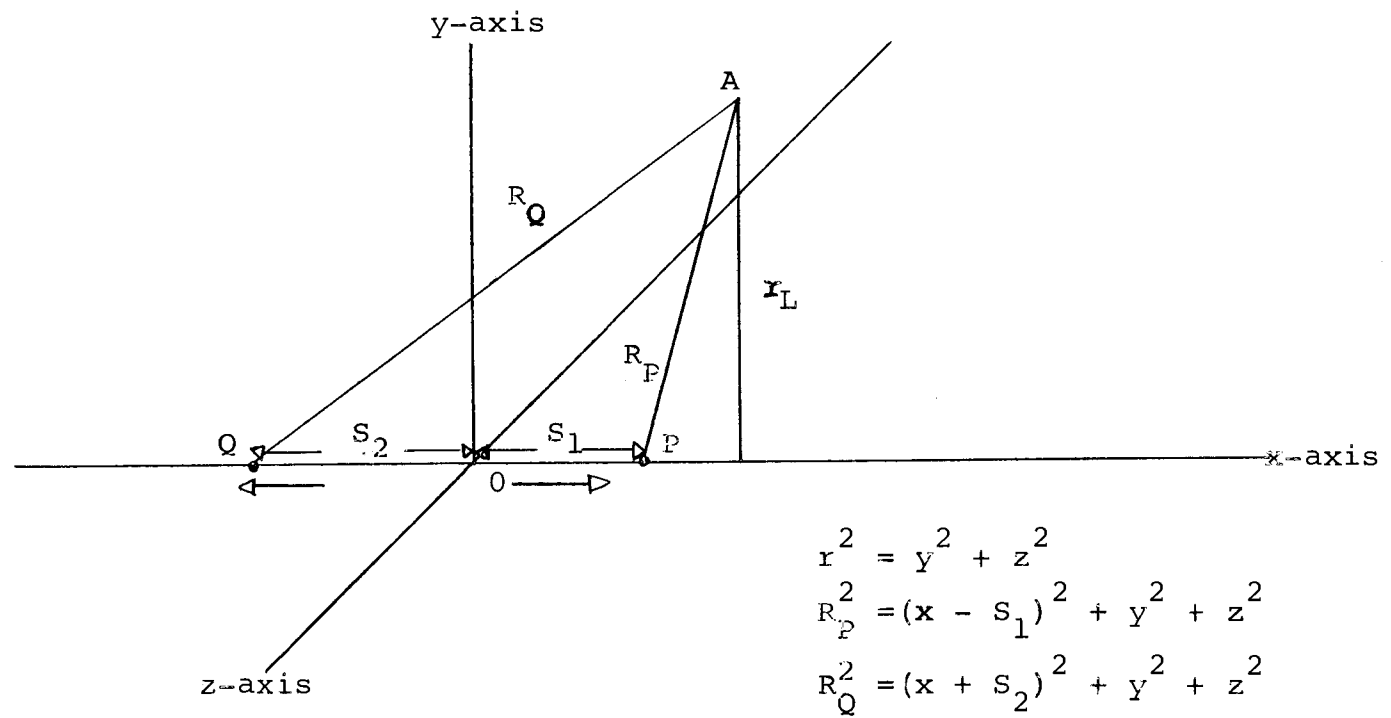


FIGURE 9

Geometry for the Mathematical Analog

point sources, located in the middle of the line source.

If the boundary condition is initially ignored, equations may be written which express the electric field intensity at a point A. The total field will be the vector sum of the fields associated with the line source and the two point sources. Using the symbols defined in Figure 9, the contribution of the line source at point A is:

$$\vec{E}_L = K_L \vec{a}_L / r_L. \quad (1)$$

Similarly, the field components at A due to the two point sources are:

$$\vec{E}_P = K_P \vec{a}_P / R_P^2 \quad (2)$$

$$\vec{E}_Q = K_Q \vec{a}_Q / R_Q^2. \quad (3)$$

The total field is then

$$\begin{aligned} \vec{E}_T &= \vec{E}_L + \vec{E}_P + \vec{E}_Q \\ &= K_L \vec{a}_L / r_L + K_P \vec{a}_P / R_P^2 + K_Q \vec{a}_Q / R_Q^2. \end{aligned} \quad (4)$$

Insertion of an insulating plane boundary, which contains point A and is parallel to the xz plane, results in cancellation of the y component of the field and doubling of the x and z components.¹ These components may be written:

¹As a consequence of the image charge concept (10, p.51).

$$E_x = 2K_P(x-s_1)/R_P^3 + 2K_Q(x+s_2)/R_Q^3 \quad (5)$$

$$E_z = 2K_L z/r_L^2 + 2K_P z/R_P^3 + 2K_Q z/R_Q^3. \quad (6)$$

The field potential at point A can be calculated as a line integral of the electric field intensity from point A to the reference point B:

$$\begin{aligned} V_{AB} &= \int_A^B \vec{E} \cdot d\vec{l} \\ &= \left[K_L \ln(r^2) - 2K_P/R_P - 2K_Q/R_Q \right] \Big|_B \\ &\quad \left[K_L \ln(r^2) - 2K_P/R_P - 2K_Q/R_Q \right] \Big|_A. \end{aligned} \quad (7)$$

Visual inspection of this equation does not readily indicate the waveform characteristics. Numerical solutions are suited to the use of a digital computer. The resultant waveform of a set of numerical solutions is shown in Figure 10. Comparison of this waveform to the monopolar waveform of Figure 3 (bottom trace) indicates that this approach should yield the desired correlations.

The convenience of the mathematical approach is lessened by the fact that the equation in this form (Equation 6) relates the potential at a point to the geometry. In other words, to simulate a set of myoelectric waveforms, one must choose a set of geometrical parameters and check

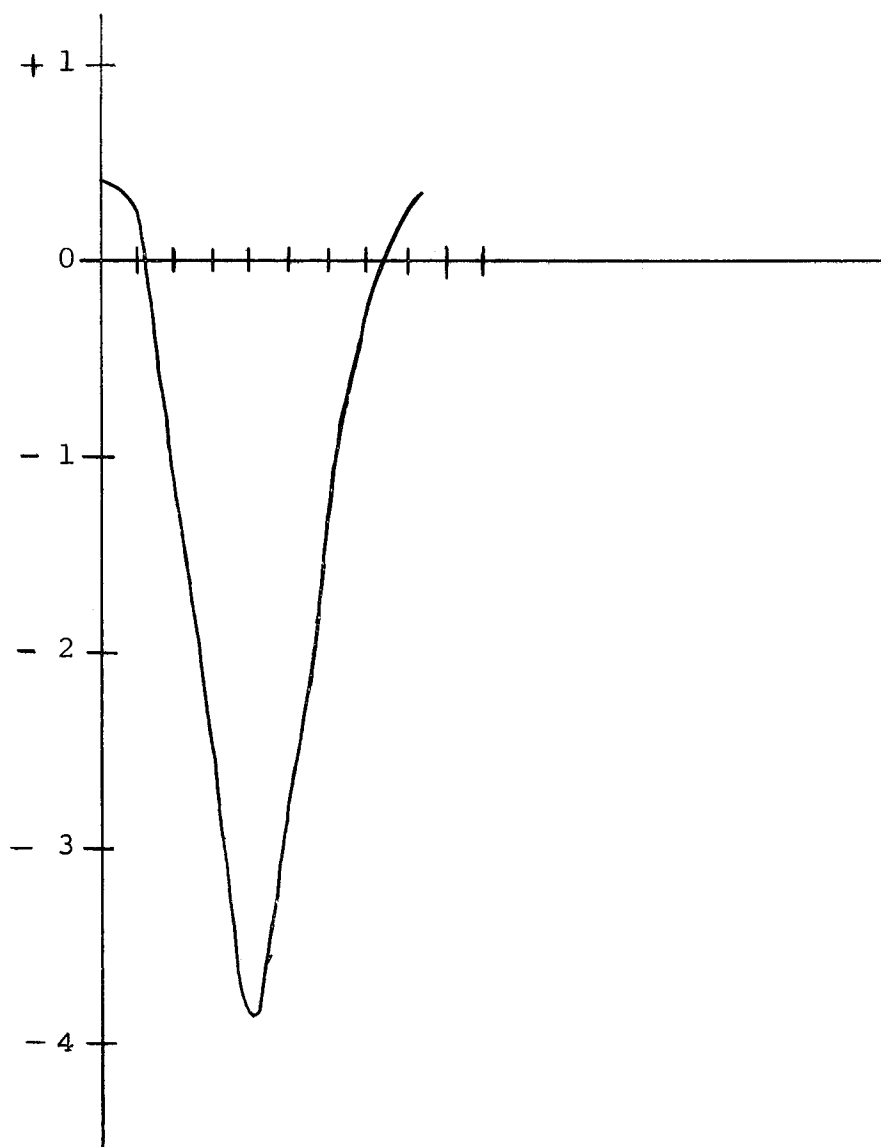


FIGURE 10

Typical Waveform Generated
by the Mathematical Analog

the numerical solutions to obtain the correlations. This procedure involves guesswork, resulting in correlations (even with the aid of a computer) that are time consuming and costly.

There is one salient difference between the waveforms observed and those generated by the analog. The leading edge of a myoelectric pulse generally starts at the zero baseline; whereas, the mathematical analog waveform exhibits a discontinuity from the zero baseline to some level. This discrepancy arises from the fact that the amplitude of the current is assumed to be either zero or equal to some constant.

For myoelectric phenomena, a risetime must be allotted for the depolarization and repolarization mechanisms to switch the current from zero to the maximum value. From Figure 8, an estimate of the risetime may be inferred to be on the order of one millisecond. Since the waveform in Figure 8 is concerned with a point on the muscle fibre membrane remote from the motor end plate, this estimate may not be strictly valid.

Similar statements may be given in reference to the trailing edge of the myoelectric pulse and an associated

falltime.

In view of the difficulties associated with the mathematical analog and the limited funds available, the electrolytic tank analog was developed to overcome some of the limitations of the mathematical analog. The chief advantage of the electrolytic tank analog is that the waveforms are generated and displayed in seconds. The same assumptions apply to the electrolytic tank analog as the mathematical one, except both the point and line sources will have a non-zero diameter. The motor unit properties may be more closely approximated by a non-zero source diameter; consequently, another parameter will be introduced into the geometric scaling.

Electrolytic Tank Fabrication

Several problems attended the construction and testing of the electrolytic tank analog, the earliest of which concerned construction of an underwater mechanism. A 3/16" brass rod which served as the line source was suspended within a wooden framework. Two 1/4" OD Delrin rings with a wire band fixed around each were fabricated to slide on the brass rod. Power was supplied to rings by

means of a small flexible insulated wire which also provided for mechanical translation of the rings. Consequently, the rings served as the traveling point sources.

The small wire was ultimately attached to a pulley which was fixed to the shaft of a potentiometer. The position of the potentiometer electrically controlled the horizontal position of the oscilloscope traces. As a result, a linear relationship was established between ring position and trace position.

Small brass machine screws (#4-40 Flathead) were suspended from a phenolic board to sample the potentials at the surface of the electrolyte (tap water).

It was discovered that DC excitation of the electrolytic analog was inappropriate for the following reasons: (1) low levels of DC excitation yielded signals at the surface electrodes which were smaller than the electrode polarization potentials; and (2) higher levels of DC excitation resulted in surface electrode potentials which exceeded the dynamic range of the instrumentation.

This problem necessitated the construction of an AC carrier system. The signal flow diagram in Figure 11 indicates the components necessary for the instrumentation

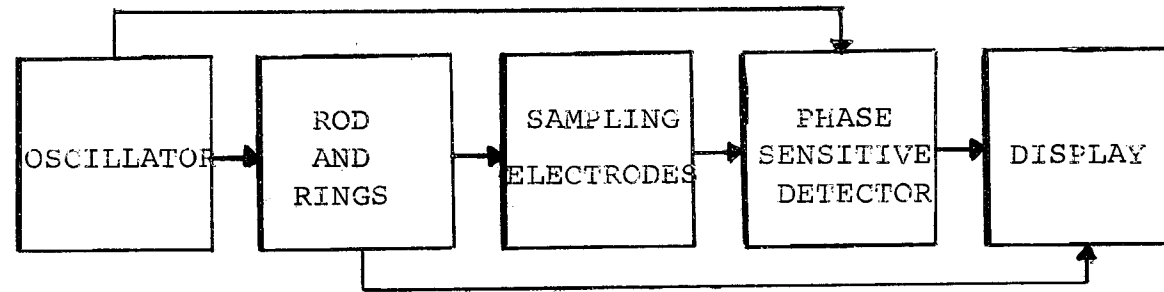


FIGURE 11

Signal Flow Diagram
for AC Carrier System

of the electrolytic tank analog.

A sample waveform as generated by the tank analog is displayed in the photograph of Figure 12, and is seen to be similar to the one generated by the mathematical analog (Figure 10). Again, the rise and fall times of the electric signals are not simulated by the analog.

Myoelectric Data Acquisition

The analog would sufficiently support the hypothesis if all of the general waveshape and time characteristics were to be reproduced. Myoelectric surface potentials must be sampled at many points simultaneously to provide enough data for formulation of the general characteristics.

Figures 13 and 14 illustrate electrode arrays which were placed on the right forearm of a subject. The differential pairs (Figure 13) were aligned parallel to the major axis of the array. Subsequently, the array was placed with its major axis approximately parallel to the muscle fibres.

Since the instrumentation was limited to eight channels, the data was taken in several runs with one channel (Channel 8) consistently sampling at one set of points to

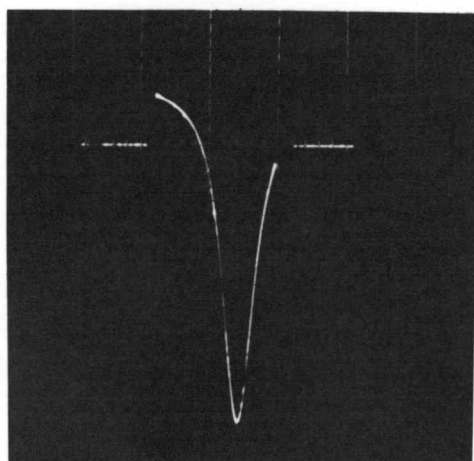


FIGURE 12

Typical Electrolytic Tank Waveform

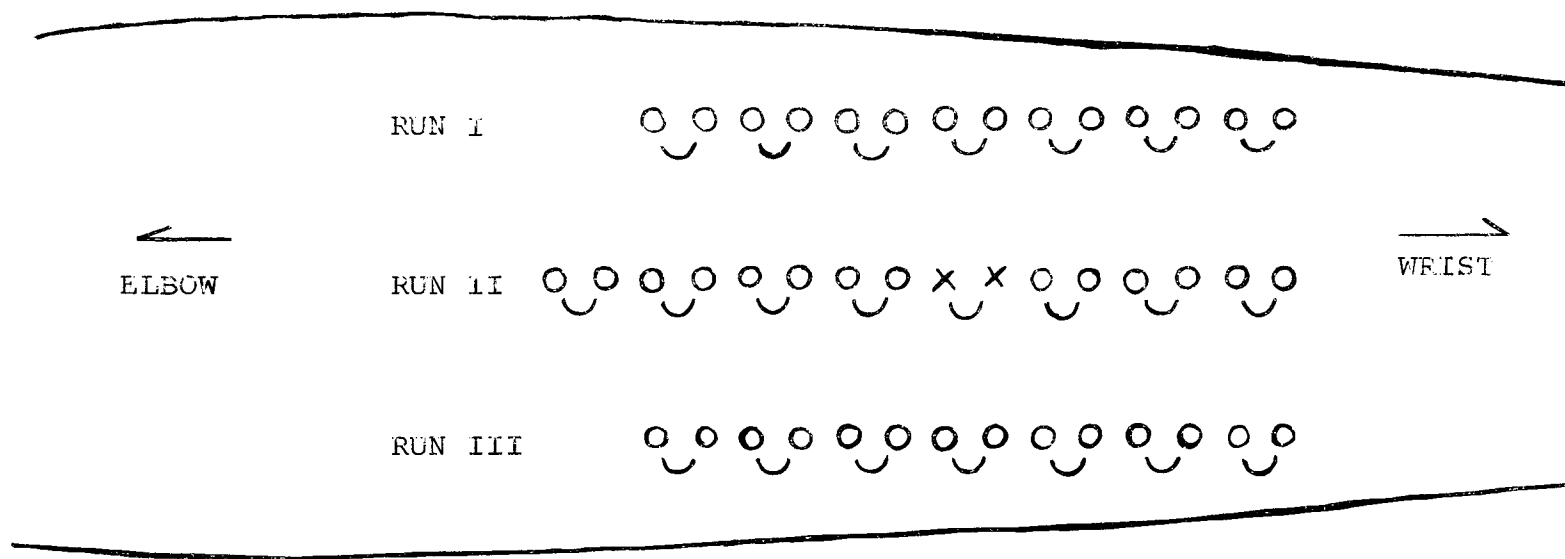


FIGURE 13

Differential Electrode Array

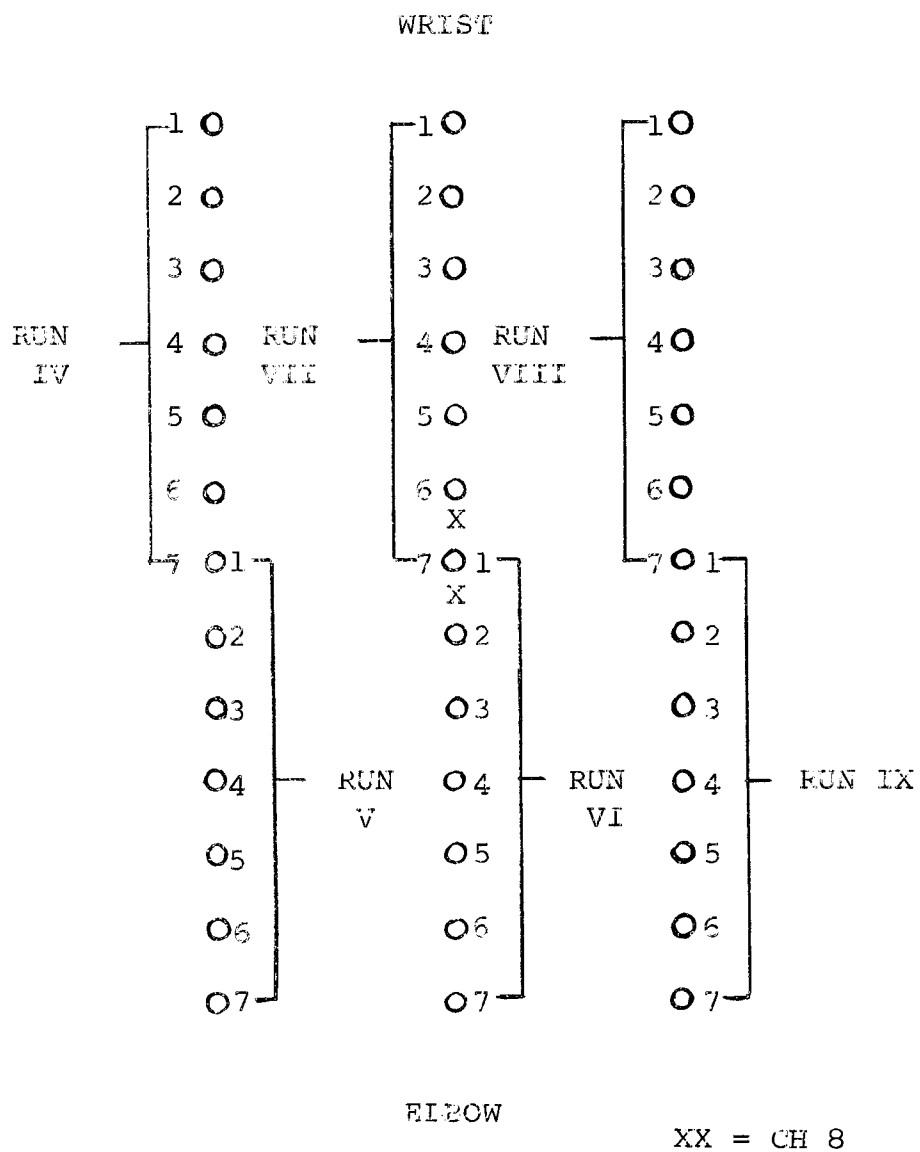


FIGURE 14

Monopolar Electrode Array

insure that the signal was not changing. Simultaneity is not preserved with this method. However, the signals were sufficiently alike (as in Figures 5 and 6) to allow correlation of different runs.

The monopolar electrode array (Figure 14) is seen to be similar to the differential electrode array. Channel 8 is the same differential pair used to preserve the identity of the signal. The monopolar electrodes are placed between the positions of the differential electrodes.

Documentation of the signals displayed on the oscilloscope was accomplished by moving film photography. The resulting 35-mm films each displayed about twenty sets of pulses in continuous traces. Several sets of pulse waveforms from each 35-mm filmstrip were enlarged and traced on transparent acetate films. The films were then overlaid such that the traced waveforms on the different sheets were superimposed. Figure 15 displays a photograph of a typical set of superimposed tracings.

Some of the superimposed waveforms in Figure 15 are distinct, whereas others are vague. Consequently, tracings were made of the average values of the superimposed waveforms (as in Figure 16).

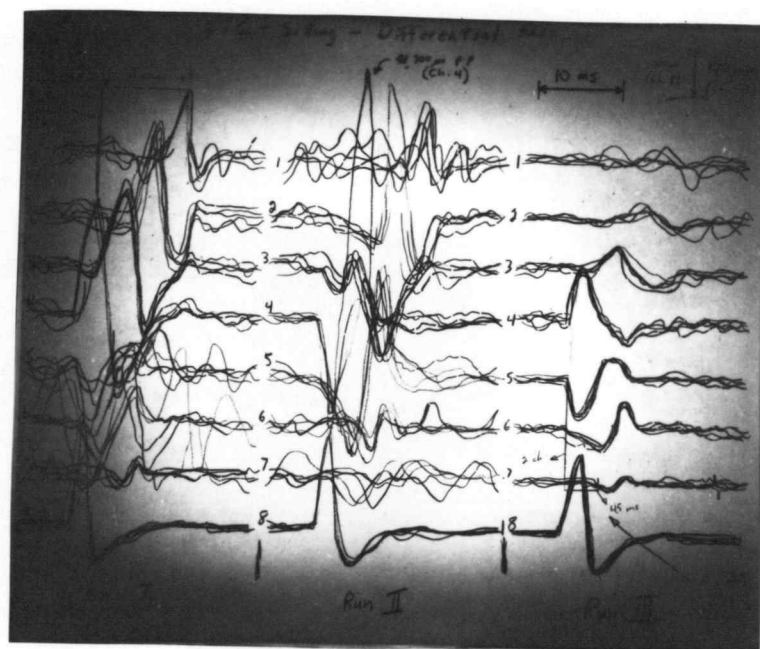


FIGURE 15

Superimposed Tracings of
Myoelectric Waveforms

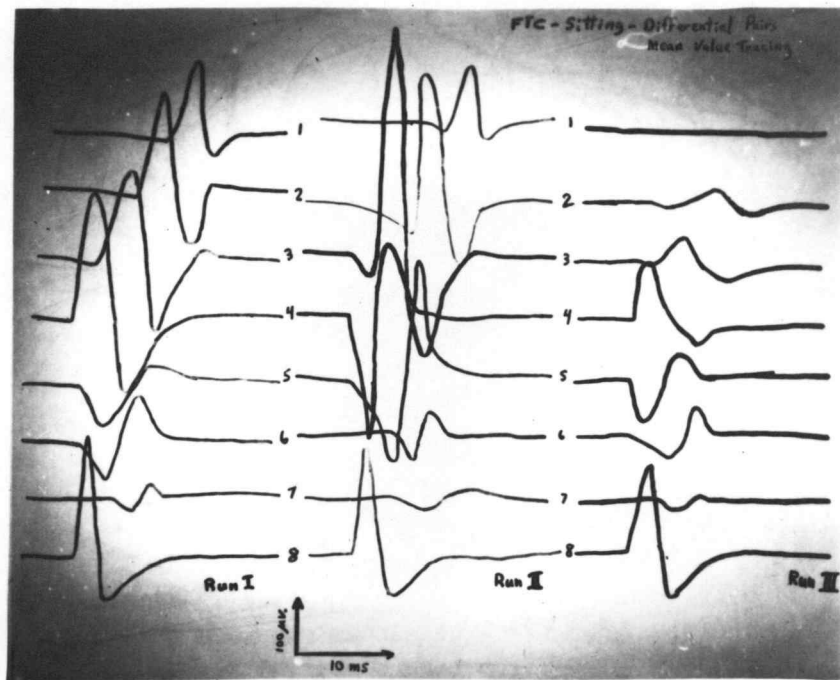


FIGURE 16

Tracing of Averaged
Differential Myoelectric Waveforms

Motor Point Location

The area of a muscle wherein the motor units are innervated is called a motor point (23). Location of this point may be deduced from a set of myoelectric data. For example, the differential waveforms displayed in Figure 15 yield the following information:

- (1) Phase reversals of the biphasic spikes sampled at certain adjacent differential pairs in a run indicate the motor point to lie somewhere between these differential pairs (as between Channels 4 and 5 in Run III, Figure 15).
- (2) Comparison of the amplitudes of signals of Runs I, II, and III indicate the point to be somewhere between Runs I and II, yet closer to Run II.

Inspection of the monopolar waveforms in Figure 17 reveals:

- (1) The location of the motor point as indicated by the earliest occurring monophasic spikes in a run is consistent with that indicated by the differential waveforms.
- (2) The effective depth of the motor unit may be estimated from the signal amplitudes between

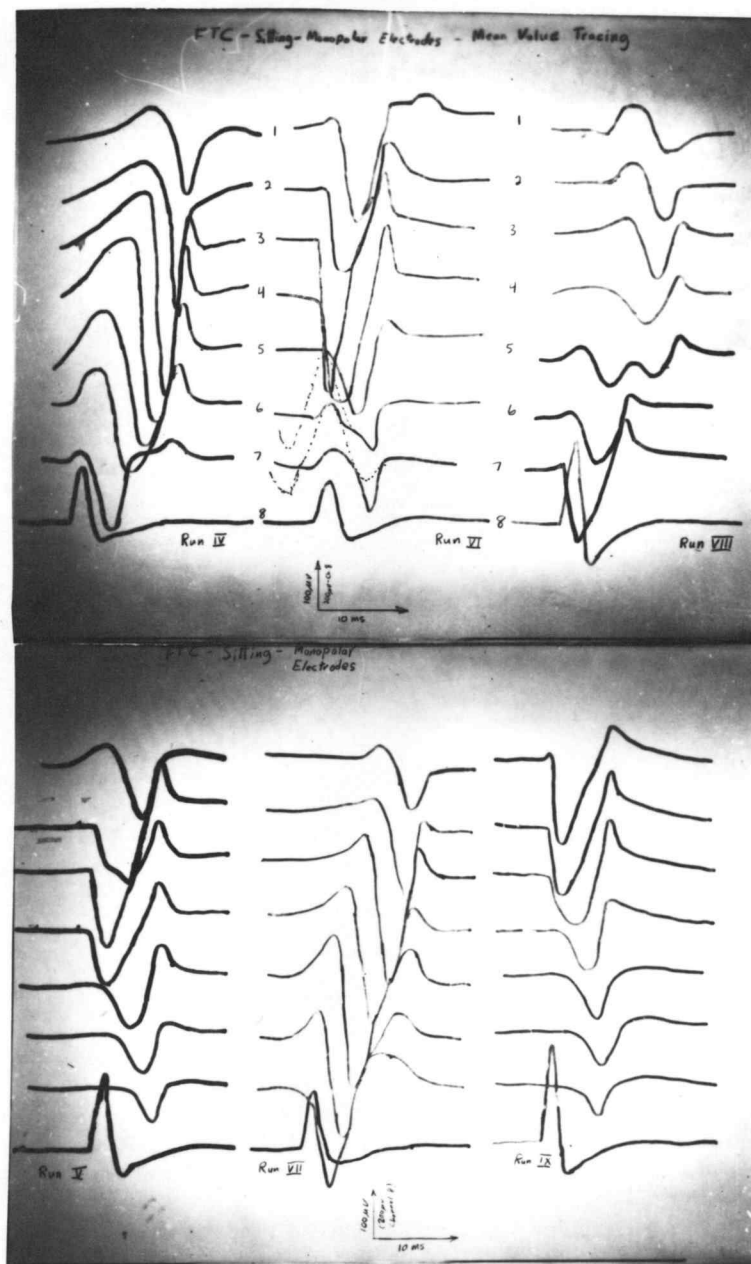


FIGURE 17

Tracing of Averaged
Monopolar Myoelectric Waveforms

runs with use of the analog concepts. The amplitude may be assumed to be an inverse function of the radial distance from the electrodes to the line source (motor unit). The amplitudes of Runs VIII and IX are about one-half the amplitudes of Runs VI and VII. Therefore, the depth must be approximately one-half the distance between the electrodes in adjacent runs.

- (3) The monopolar electrode array seems to yield better resolution in time shift than the differential pattern, due to the reduction in spacing between channels.

This information should be sufficient for establishing the geometry necessary for analog simulation of the myoelectric waveforms.

Figures 18 and 19 display superimposed tracings of myoelectric waveforms obtained with similar electrode arrays from another subject. The inconsistencies in these data are readily apparent. For example, the differential waveforms in Figure 18 show two sets of phase reversals in Run II. Many of the differential channels have no distinct waveform. There is no apparent time shift in the

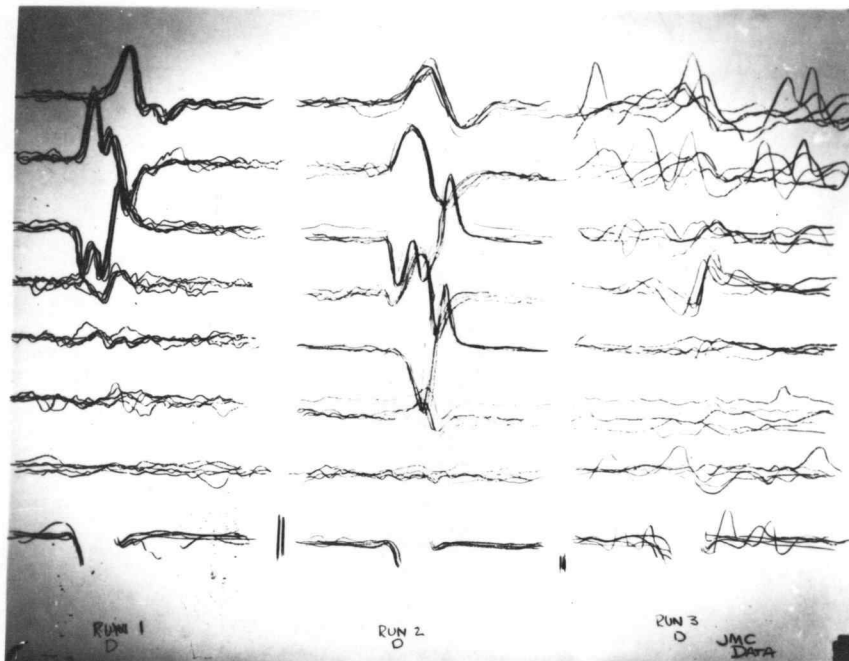


FIGURE 18

Superimposed Tracings of Differential
Myoelectric Waveforms (Subject No. 2)

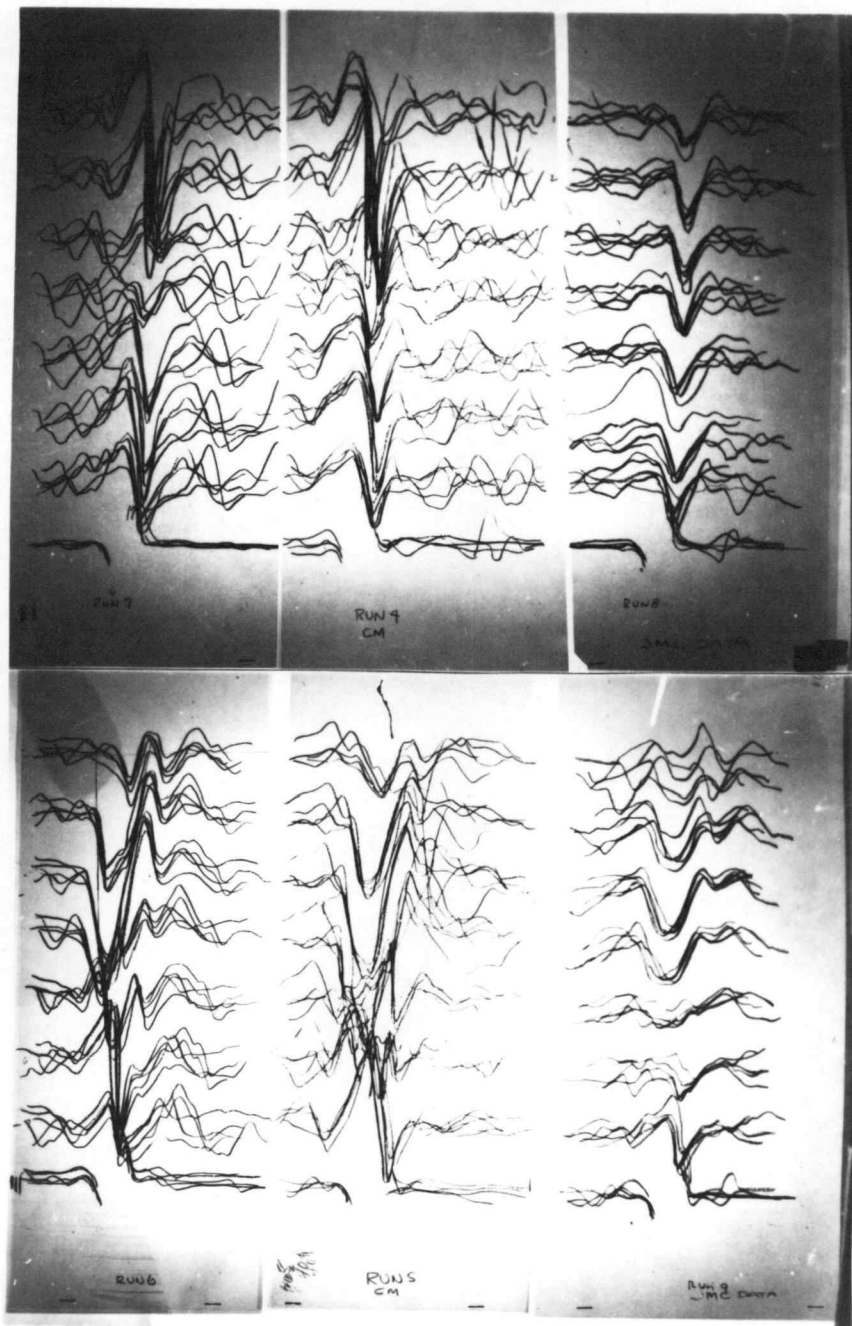


FIGURE 19

Superimposed Tracing of Monopolar
Myoelectric Waveforms (Subject No. 2)

monopolar waveforms of Figure 19. Clearly these waveforms cannot be generated by the same simple analog as the waveforms in Figures 16 and 17.

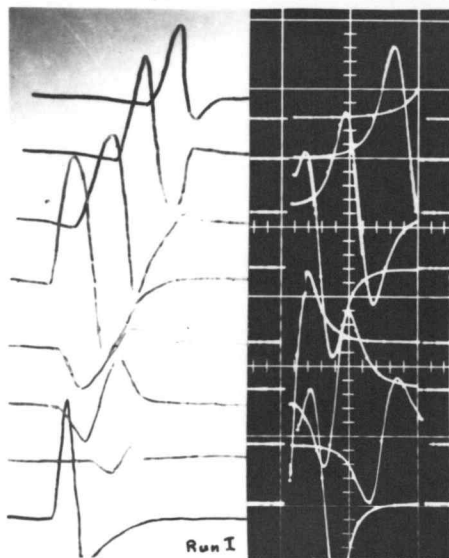
Procedure

The analog fabrication was completed with the addition of electrode patterns identical to the ones used for obtaining the myoelectric data, and with the origin centered at the indicated position of the motor point. The electrodes were spaced $3/4$ " apart; effectively scaling the analog by a factor of three. The depth of the line source was set at $5/8$ ". A switching arrangement was devised to transfer the input and output of the phase sensitive detector from channel to channel as needed.

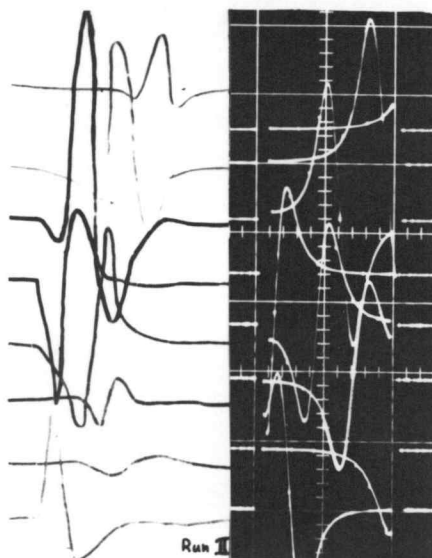
Documentation was accomplished by multiple exposures of the eight waveforms in each run using Polaroid film. Slight gaps were left in each waveform to signify the non-simulation of the rise and fall times.

Results

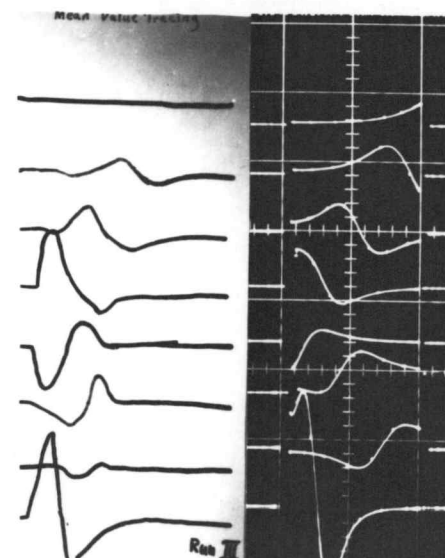
The waveforms obtained from the electrolytic tank analog are displayed in Figures 20, 21, and 22. Each set of



Run I



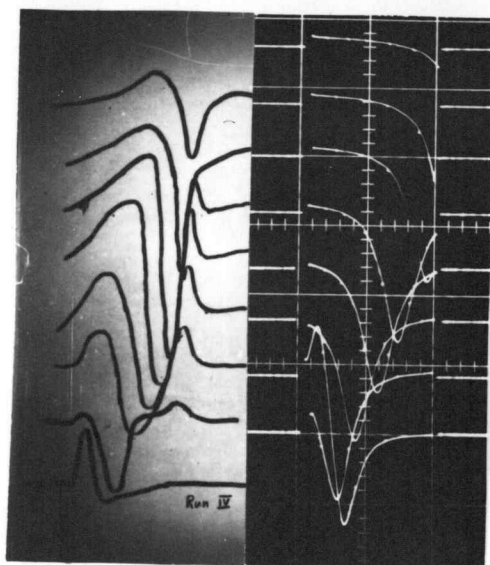
Run II



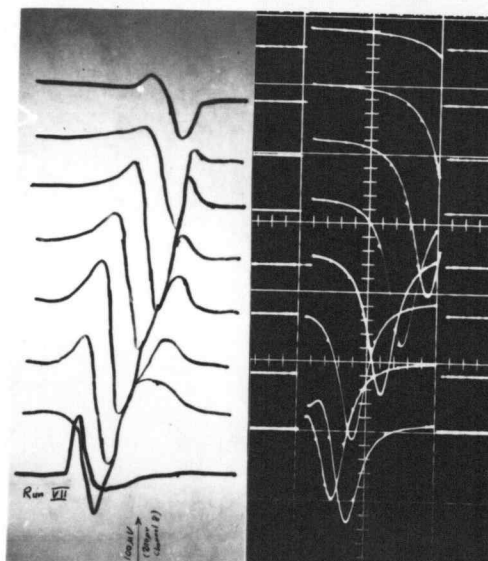
Run III

FIGURE 20

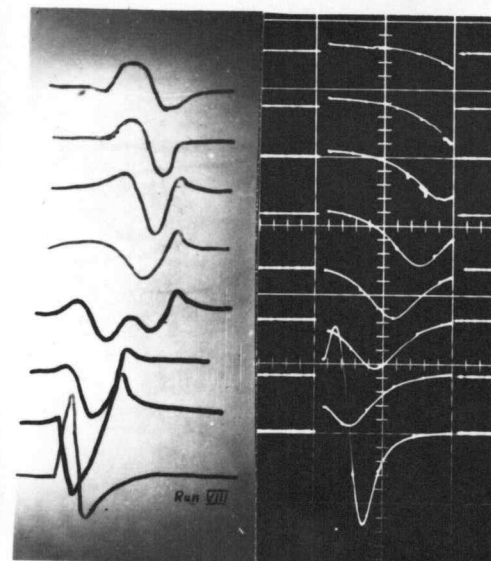
Comparison of Differential
Myoelectric and Analog Waveforms



Run IV



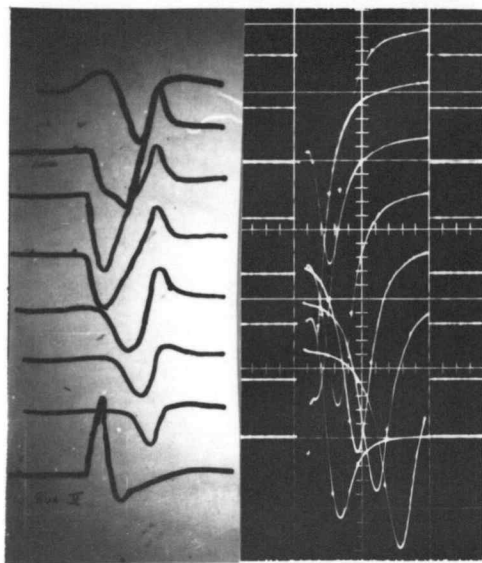
Run VII



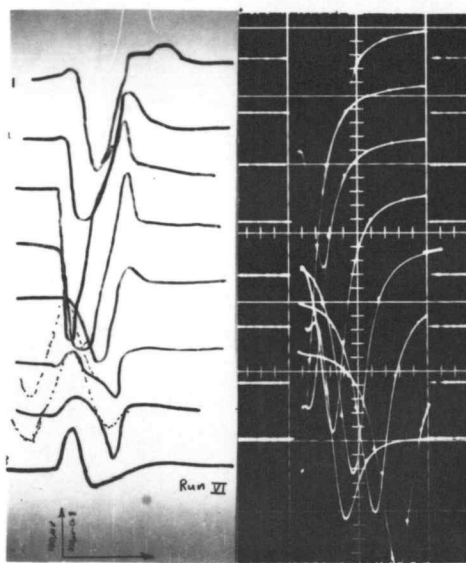
Run VIII

FIGURE 21

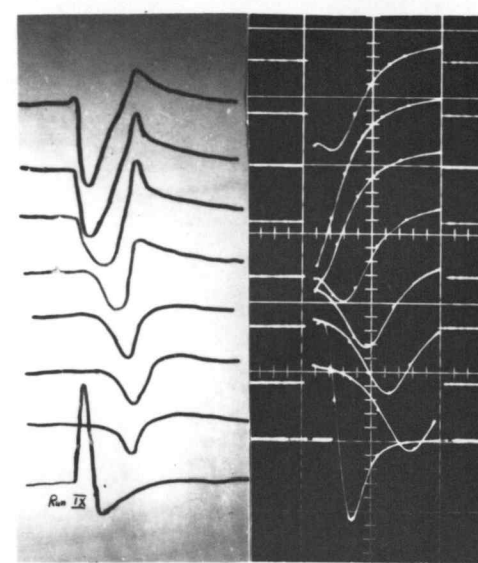
Comparison of Distal Monopolar
Myoelectric and Analog Waveforms



Run V



Run VI



Run IX

FIGURE 22

Comparison of Proximal Monopolar
Myoelectric and Analog Waveforms

analog waveforms is presented with the corresponding set of myoelectric waveforms.

In each run, the time shift relationships are the same in both the myoelectric waveforms and the analog waveforms. Perhaps the clearest example of time shift is displayed in Run VII, Figure 21. Consideration of the waveforms, relative to the electrode array (Figure 14), indicates the timeshift to be clearly a function of the distance between the point sampled and the motor point.

Phase characteristics of the analog differential waveforms (Figure 20) matched in every case the phase characteristics of the myoelectric waveforms. An excellent example of matching phase characteristics is displayed in Run III of Figure 20. The waveforms are positive phase in channels 2, 3, 4 and 8; negative phase in channels 5, 6 and 7. The amplitude characteristics are, in most cases, consistent between the comparable myoelectric and analog waveforms.

CONCLUSION

The objective was to construct an electrolytic tank

analog which would produce waveforms with characteristics similar to observed myoelectric waveforms.

This objective has been achieved as demonstrated by the waveforms in Figures 20, 21, 22. The closeness of correlation between the myoelectric and analog waveforms implies that the basic assumptions were valid at least in the first approximation.

Investigation of the rise and fall times associated with motor unit excitation and subsequent implementation of rise and fall times in the electrolytic tank analog would lead to much better analog representations of myoelectric surface phenomena. The difficulties associated with electrolytic implementation of rise and fall times may be cause for re-examination of the mathematical approach. Further pursuit of the mathematical approach might involve simultaneous solution of equations which describe the potential of several points simultaneously. Ultimately, statistical concepts may be employed to design models which would exhibit precise correlation (with variance) between model and myoelectric data.

However, more information may yet be obtained through use of the electrolytic tank analog. The convenience of

this approach would be greatly enhanced if all eight channels were to be recorded simultaneously. This method would require the construction of seven additional phase sensitive detectors. The methods of documentation and tracing of the myoelectric data are awkward, requiring considerable time to obtain an acceptable set of data. Use of methods such as in Figures 5 and 6 are much more convenient, but they would require some method of advance triggering to retain the leading edges of the myoelectric waveforms.

Use of such methods would aid in placement of electrode systems as eight channels of repetitively displayed waveforms could be monitored. Changes in waveform patterns could be correlated with changes in electrode placement, thus allowing the documentation of only the desired waveform displays.

This work should be viewed as a first rough approximation to simulation of myoelectric surface potentials with an electrolytic tank analog. It is hoped that these results will lead to further experimentation in this area.

BIBLIOGRAPHY

1. Bouman, H. D. and A. L. Woolf (eds.). The Utrecht Symposium on the Innervation of Muscle. Baltimore, Maryland, Williams and Wilkins, 1960. 223 p.
2. Bourne, G. H. (ed.). The structure and function of muscle. New York, Academic Press, 1960. 3 vols.
3. Buchthal, Fritz. The functional organization of the motor unit. In: The Utrecht Symposium on the Innervation of Muscle, University of Utrecht, 1957. Baltimore, Maryland, Williams and Wilkins, 1960. p. 13-16.
4. Buchthal, Fritz. The general concept of the motor unit. Association for Research in Nervous and Mental Diseases 38:1. 1960.
5. Christensen, Erna. Topography of terminal motor nerve innervation in striated muscles from stillborn infants. In: The Utrecht Symposium on the Innervation of Muscle, University of Utrecht, 1957. Baltimore, Maryland, Williams and Wilkins, 1960. p. 17-30.
6. Davis, J. F. Manual of surface electromyography: Laboratory Psychology Study Mimeograph. Montreal, Canada, McGill University, Allen Memorial Institute Psychiatry, 1952. 145 p.
7. Fischer, Ernst. Physiology of skeletal muscle. In: Electrodiagnosis and Electromyography. 2d. ed. New Haven, Connecticut, Elizabeth Licht, 1961. p. 66-112.
8. Forbes, A. and A. M. Grass. Simple direct-coupled amplifier for action potentials. Journal of Physiology 91:31-35. 1937.
9. Goodgold, J. and J. Moldaver. Changes in electromyographic wave forms in relation to variation in type and position of electrode. Archives of Physical Medicine 36:627-630. 1955.

10. Jordan, Edward C. Electromagnetic waves and radiating systems. Englewood Cliffs, N. J., Prentice-Hall, 1960. 710 p.
11. Kobrinsky, A. Y. Bioelectric control of prosthetic devices. vol. 30 no. 7. U.S.S.R., Herald Academy of Science, 1960. (Official Technical Service Translation 61 11074 B 50). (Cited in G. Stone, Ref. #20).
12. Kobrinsky, A. Y. Russia's amazing electronic hand. Electronics Illustrated 6:62-63. 1963.
13. Licht, Sidney (ed.). Electrodiagnosis and electromyography. 2nd. ed. New Haven, Connecticut, Elizabeth Licht, 1961. 470 p.
14. Lockhart, R. W. and W. Brandt. Length of striated muscle fibers. Journal of Anatomy 72:470. 1938.
15. Michael, R. R. Myoelectric surface potentials for machine control. Conference Paper. Spokane, Washington, The Institute of Electrical and Electronics Engineers, 1963. 4 numb. leaves.
16. Nickel, V. L. Control systems for externally powered orthotics. (Abstract) Institute of Radio Engineers Transactions Bio-Medical Electronics BME-8(4):266. October 1961.
17. Rogers, W. M. and H. O. Parrack. Electronic apparatus for recording and measuring electrical potentials in nerve and muscle. Proceedings of the Institute of Radio Engineers 32:738-742. December 1944.
18. Rogoff, Joseph B. and Stuart Reiner. Electrodiagnostic apparatus. In: Electrodiagnosis and Electromyography. 2d. ed. New Haven, Connecticut, Elizabeth Licht, 1961. p. 24-65.
19. Rosenblueth, Arturo. The transmission of nerve impulses at neuroeffector junctions and peripheral synapses. New York, John Wiley and Sons, Massachusetts Institute of Technology, 1950. 325 p.

20. Stone, G. Some considerations in the design of externally powered upper-extremity prosthesis. In: Human Factors in Technology, New York, McGraw-Hill, 1963. p. 411-424.
21. Suckling, E. E. Bioelectricity. New York, McGraw-Hill, 1961. 233 p.
22. Walls, E. W. The microanatomy of muscle. In: The Structure and Function of Muscle, vol. 1. New York, Academic Press, 1960. p. 21-61.
23. Walthard, Karl M. and Michael Tchicaloff. Motor points. In: Electrodiagnosis and Electromyography. 2d. ed. New Haven, Connecticut, Elizabeth Licht, 1961. p. 153-170.
24. Weltman, G., H. Garth, and J. Lyman. A myoelectric system for training functional dissociation of muscles. Archives of Physical Medicine 43:534-7. 1962.
25. Weltman, G., et al. Myoelectric servo-boost system. Los Angeles, University of California, Spacelabs, Inc. and Biotechnology Laboratory, 1962.